


SHORT COMMUNICATION



Morpholine-based chalcones as dual-acting monoamine oxidase-B and acetylcholinesterase inhibitors: synthesis and biochemical investigations

Rani Sasidharan^{a,b#}, Bo Hyun Eom^{c#}, Jeong Hyun Heo^{c#}, Jong Eun Park^c, Mohamed A. Abdelgawad^{d,e}, Arafa Musa^{f,g}, Nicola Gambacorta^h, Orazio Nicolotti^h, Sreedharannair Leelabaiamma Manju^b, Bijo Mathew^{i*} and Hoon Kim^c 

^aCollege of Pharmaceutical Science, Government T.D. Medical College, Alappuzha, India; ^bOrganic Chemistry Division, SAS, VIT University, Vellore, India; ^cDepartment of Pharmacy, and Research Institute of Life Pharmaceutical Sciences, Suncheon National University, Suncheon, Republic of Korea; ^dPharmaceutical Chemistry Department, College of Pharmacy, Jouf University, Sakaka, Saudi Arabia; ^ePharmaceutical Organic Chemistry Department, Faculty of Pharmacy, Beni-Suef University, Beni Suef, Egypt; ^fDepartment of Pharmacognosy, College of Pharmacy, Jouf University, Sakaka, Saudi Arabia; ^gDepartment of Pharmacognosy, Al-Azhar University, Cairo, Egypt; ^hDipartimento di Farmacia—Scienze del Farmaco, Università degli Studi di Bari “Aldo Moro”, Bari, Italy; ⁱDivision of Drug Design and Medicinal Chemistry Research Lab, Department of Pharmaceutical Chemistry, Ahalia School of Pharmacy, Palakkad, India

ABSTRACT

Nine compounds (**MO1–MO9**) containing the morpholine moiety were assessed for their inhibitory activities against monoamine oxidases (MAOs) and acetylcholinesterase (AChE). Most of the compounds potently inhibited MAO-B; **MO1** most potently inhibited with an IC_{50} value of $0.030\ \mu\text{M}$, followed by **MO7** ($0.25\ \mu\text{M}$). **MO5** most potently inhibited AChE ($IC_{50} = 6.1\ \mu\text{M}$), followed by **MO9** ($IC_{50} = 12.01\ \mu\text{M}$) and **MO7** most potently inhibited MAO-A ($IC_{50} = 7.1\ \mu\text{M}$). **MO1** was a reversible mixed-type inhibitor of MAO-B ($K_i = 0.018\ \mu\text{M}$); **MO5** reversibly competitively inhibited AChE ($K_i = 2.52\ \mu\text{M}$); and **MO9** reversibly non-competitively inhibited AChE ($K_i = 7.04\ \mu\text{M}$). **MO1**, **MO5** and **MO9** crossed the blood–brain barrier, and were non-toxic to normal VERO cells. These results show that **MO1** is a selective inhibitor of MAO-B and that **MO5** is a dual-acting inhibitor of AChE and MAO-B, and that both should be considered candidates for the treatment of Alzheimer’s disease.

ARTICLE HISTORY

Received 16 September 2020
Revised 21 October 2020
Accepted 22 October 2020

KEYWORDS

Morpholine-containing chalcone; monoamine oxidase; acetylcholinesterase; dual-acting inhibitor; Docking analysis


1. Introduction

Due to the extreme complexities of brain systems and their diverse dysfunctions, research focus is being directed towards the design of multi-target directed ligands (MTDLs)¹. In fact, it has been suggested that functional equilibrium of brain after a neurologic disorder is unlikely to be achieved by focussing on a single molecular target². The major challenge presented by the development of MTDLs is to preserve balance between the effects drugs have by acting at their individual molecular targets³. On the other hand, some ligands can target two or more specific entities within numerous biological networks. The likelihood of successful MTDL design can be enhanced by considering the design of molecular scaffolds via suitable molecular hybridisation and by understanding the pathophysiologies of multifaceted diseases. The design process can be accelerated by selecting pharmacophores based on pre-clinical studies, emphasising structure–activity relationships (SARs) and by performing *in silico*-based virtual screening⁴.

Monoamine oxidases (MAOs) play prominent roles in the inactivations of various biogenic amines in central and peripheral tissues. The isoenzymes of MAO-A and MAO-B are considered major


therapeutic targets in various neuropsychiatric illnesses and neurodegenerative disorders like Alzheimer’s disease (AD) and Parkinson’s disease (PD)⁵. During the degradations of various biogenic neurotransmitters catalysed by MAO-A and MAO-B, hydrogen peroxide and reactive oxygen species (ROS) are produced as major by-products, which might cause oxidative damage in brain tissues. MAO inhibitors are considered potential neuroprotective agents and up-regulating agents for neurotransmitter amines⁶. Numerous studies have documented that selective and reversible/irreversible MAO-B inhibitors are likely to play pivotal roles in AD-related therapeutic strategies. Acetylcholinesterase (AChE) and butyrylcholinesterase (BChE) inhibitors also play significant roles in the maintenance of cholinergic functions and are used to provide symptomatic relief in AD. Over the past two decades, many researchers have tried to develop multi-acting MAO-B and AChE/BChE inhibitors^{7–10}.

Morpholine is a tetrahydro-1,4-oxazine with a saturated heterocyclic ring and provides a promising developmental starting point due to its biological profile with metabolic stability. The presence of a heteroatom like oxygen or nitrogen facilitates hydrogen bonding, and thus, interactions with enzymes, and the presence

CONTACT Hoon Kim  hoon@sunchon.ac.kr  Department of Pharmacy, and Research Institute of Life Pharmaceutical Sciences, Suncheon National University, Suncheon 57922, Republic of Korea; Bijo Mathew  bijomathew@aims.amrita.edu  Department of Pharmaceutical Chemistry, Amrita School of Pharmacy, Amrita Vishwa Vidyapeetham, AIMS Health Sciences Campus, Kochi-682 041, India; Sreedharannair Leelabaiamma Manju  slmanju@vit.ac.in  Organic Chemistry Division, SAS, VIT University, Vellore, India

[#]These authors contributed equally to this work.

*Department of Pharmaceutical Chemistry, Amrita School of Pharmacy, Amrita Vishwa Vidyapeetham, AIMS Health Sciences Campus, Kochi-682 041, India.

 Supplemental data for this article can be accessed [here](#).

© 2021 The Author(s). Published by Informa UK Limited, trading as Taylor & Francis Group.

This is an Open Access article distributed under the terms of the Creative Commons Attribution License (<http://creativecommons.org/licenses/by/4.0/>), which permits unrestricted use, distribution, and reproduction in any medium, provided the original work is properly cited.

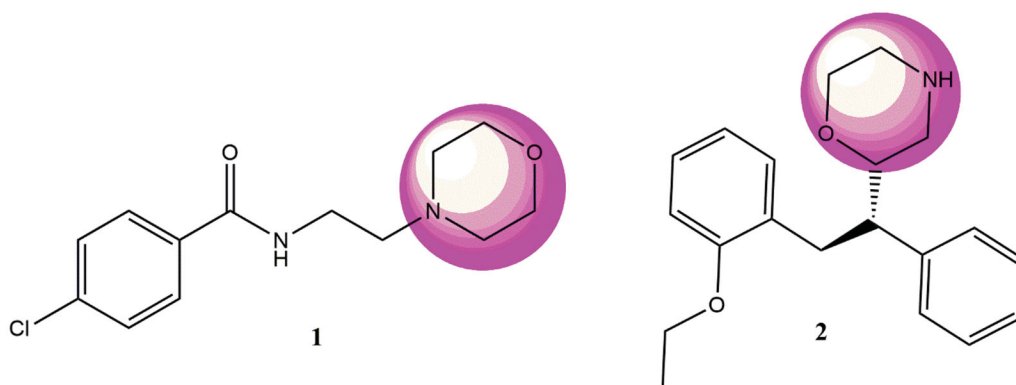


Figure 1. Morpholine-containing, CNS active, FDA approved drugs. 1, moclobemide; 2, reboxetine.

of electron-deficient atoms may also impart hydrophobic interactions with morpholine. From the synthetic perspective, various molecular scaffolds have been added to morpholine by replacing its secondary nitrogen¹¹. Moclobemide (1) and reboxetine (2) (both antidepressants) provide examples of FDA-approved drugs containing the morpholine moiety (Figure 1). These drugs reversibly inhibit MAO-A and selectively inhibit norepinephrine reuptake in the central nervous system (CNS), and thus, block the human $\alpha_4\beta_2$ nicotinic acetylcholine receptor. In addition, more than 20 drugs containing the morpholine moiety have been FDA approved; they include mycophenolate mofetil (an immunosuppressant), linezolid and finafloxacin (antibiotics), gefitinib (an anti-neoplastic and epidermal growth factor inhibitor), rivaroxaban (an anticoagulant and factor Xa inhibitor), and eteplirsen, which is used to treat Duchenne muscular dystrophy¹². Considering the importance of morpholine nucleus, it is worthwhile to design morpholine derived compounds of medicinal chemistry interest.

The chalcones framework is considered an excellent starting point for the design for MAO-B and AChE enzyme inhibitors^{13–15}. The presence of an α - β unsaturated ketone and three rotatable bonds in chalcones can provide different bonding orientations¹⁶. The literature amply demonstrates that most chalcones are potent, reversible and selective MAO-B inhibitors¹⁷. In addition, the presence and orientation of various electron-donating and withdrawing groups on the phenyl/heteroaryl **A** and **B** rings of chalcones can impart electrophilic character to the Michael acceptor present. The introductions of electron-donating/lipophilic halogens onto the phenyl **B** ring of chalcones have resulted in the syntheses of highly selective MAO-B inhibitors^{18–27}. Many studies have reported that the presence of various alkylamino groups on the **A** ring provides AChE inhibitory activity^{28–31}. The FDA-approved drugs like flurbiprofen and rivastigmine linked with chalcone moiety were developed as selective ChE/MAO-B inhibitors for the prophylactic agents for AD³². The design strategy of the current study is depicted in Figure 2 and the synthetic route is shown in Scheme 1. A recent study showed that the presence of a pendant morpholine ring on the chalcone **A** ring favoured hMAO-B inhibitory activity^{33,34}. The difference in MAO-B inhibition profiles became more obvious when chalcone **B** ring was substituted using a fluoro or trifluoromethyl group³³.

2. Results and discussion

2.1. Chemistry

Morpholine-containing α,β -unsaturated ketones were prepared by condensation between various aromatic/*para* substituted

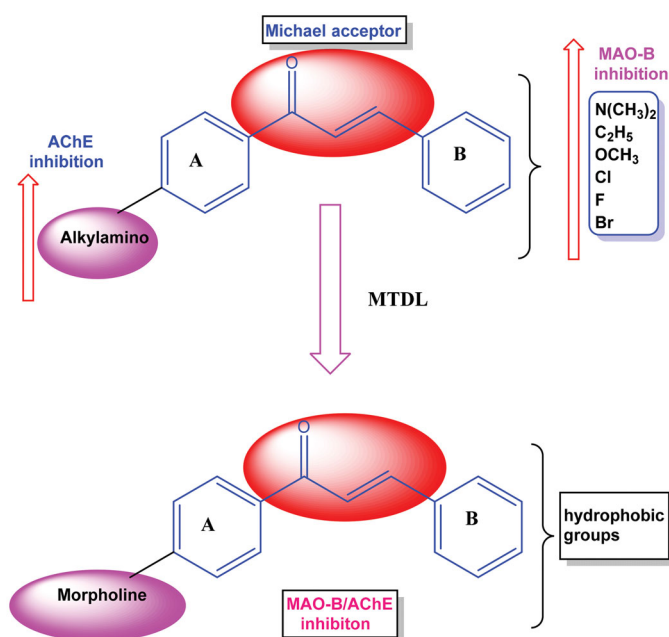


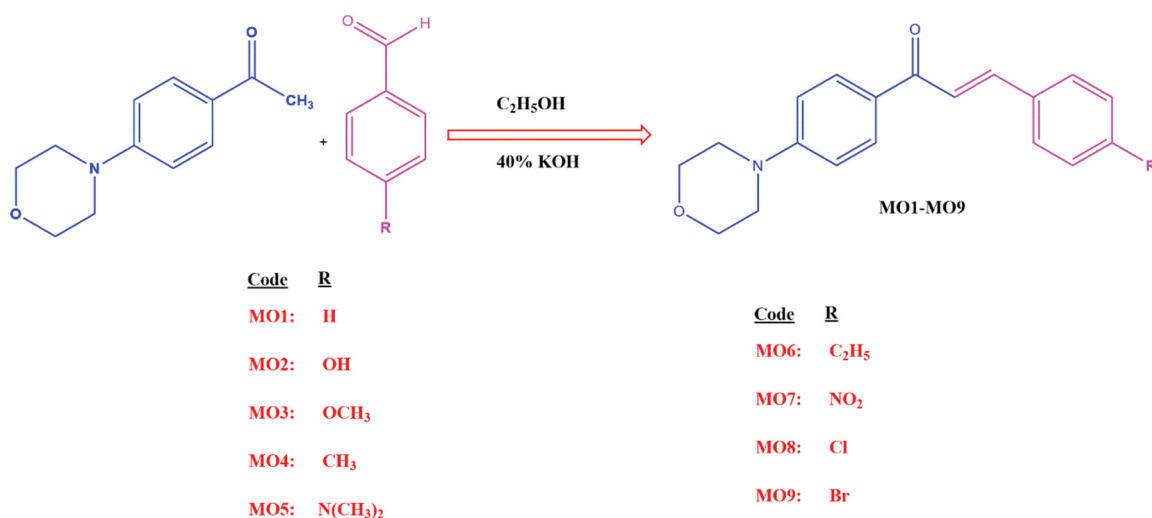
Figure 2. MTDL design of MAO-B and AChE inhibitors.

aldehydes and 4-morpholine acetophenone in the presence of an alcoholic basic medium³³. The ^1H NMR showed that the ring protons N-CH₂ and O-CH₂ of morpholine ring resonated at 3.32–3.31 and 3.75–3.88 ppm as triplets, respectively. The large coupling constant ($J=15\text{ Hz}$) value of H α and H β protons confirmed the *trans* configuration of the morpholine chalcones. The deshielded values between 186.88–186.07 in ^{13}C -NMR clearly evidenced the formation of sp^2 carbonyl functional group of α,β -unsaturated ketones. The identities of the compounds were determined by ^1H -NMR, ^{13}C -NMR and Mass spectrometry (Supplementary materials).

2.2. Analysis of enzyme inhibitory activities

2.2.1. Inhibitory activities

In this study, nine morpholine-based compounds (**MO1–MO9**) were analysed with respect to their abilities to inhibit MAO-A, MAO-B and AChE. Most of the compounds inhibited MAO-B by $\sim 50\%$ at $1.0\ \mu\text{M}$, except **MO3** and **MO5** (Table 1). Compound **MO1** most potently inhibited MAO-B ($\text{IC}_{50} = 0.030\ \mu\text{M}$), followed by **MO7**, **MO8**, **MO4**, **MO9**, **MO6**, **MO2**, **MO3** and **MO5** ($\text{IC}_{50} = 0.25, 0.32, 0.33, 0.36, 0.64, 0.70, 1.01$ and $1.31\ \mu\text{M}$, respectively). In



Scheme 1. The synthetic route used to produce the target compounds (MO1–MO9).

Table 1. Inhibitions of MAO-A, MAO-B, and AChE by MO1–MO9^a

Compounds	Residual activities (%)				IC ₅₀ (μM)				
	MAO-A (10 μM)	MAO-B (1.0 μM)	AChE (10 μM)	BChE (10 μM)	MAO-A	MAO-B	AChE	BChE	SI ^b
MO1	94.2 ± 0.62	38.1 ± 9.50	53.4 ± 0.99	62.85 ± 2.97	>40	0.030 ± 0.062	16.1 ± 2.24	>40	>1333.3
MO2	93.8 ± 1.34	54.5 ± 5.28	72.3 ± 1.34	63.55 ± 3.30	>40	0.70 ± 0.23	30.2 ± 3.24	>40	> 57.1
MO3	91.0 ± 3.17	79.9 ± 5.28	79.3 ± 2.82	56.78 ± 2.97	>40	1.01 ± 0.08	>40	>40	>39.6
MO4	70.2 ± 1.24	49.0 ± 1.45	66.0 ± 8.79	80.30 ± 6.43	25.8 ± 1.58	0.33 ± 0.03	28.42 ± 0.02	>40	78.2
MO5	88.1 ± 3.43	58.6 ± 3.39	34.5 ± 9.51	60.86 ± 1.07	>40	1.31 ± 0.26	6.1 ± 0.0048	18.09 ± 0.38	>30.5
MO6	12.3 ± 1.58	64.1 ± 1.37	76.9 ± 3.54	70.96 ± 0.36	8.7 ± 1.32	0.64 ± 0.04	>40	>40	13.6
MO7	−16.5 ± 4.53	26.1 ± 5.44	65.3 ± 1.55	70.21 ± 4.76	7.1 ± 0.41	0.25 ± 0.05	20.48 ± 1.10	24.83 ± 0.34	28.4
MO8	83.7 ± 4.02	34.6 ± 5.44	50.6 ± 3.61	74.61 ± 0.73	>40	0.32 ± 0.16	12.07 ± 1.18	>40	>125.0
MO9	79.8 ± 1.54	51.3 ± 2.42	50.4 ± 2.42	70.21 ± 5.50	>40	0.36 ± 0.16	12.01 ± 2.13	>40	>111.1
Toloxatone					1.08 ± 0.025	—			
Lazabemide					—	0.063 ± 0.015			
Clorgyline					0.007 ± 0.00070	—			
Pargyline					—	0.028 ± 0.0043			
Tacrine							0.27 ± 0.019	0.060 ± 0.0022	

^aValues above are the means ± SEs of duplicate or triplicate experiments.

^bSI = IC₅₀ of MAO-A/IC₅₀ of MAO-B.

AChE values were determined after pre-incubation compounds and enzymes for 15 min.

addition, **MO5** most potently inhibited AChE (IC₅₀ = 6.1 μM), followed by **MO9** and **MO8** (IC₅₀ = 12.01 and 12.07 μM, respectively). **MO7** most potently inhibited MAO-A (IC₅₀ = 7.1 μM), followed by **MO6** (IC₅₀ = 8.7 μM). **MO5** most potently inhibited BChE (IC₅₀ = 18.09 μM), with weaker inhibitory activity compared to AChE, followed by **MO7** (IC₅₀ = 24.83 μM) (Table 1).

Morpholine-containing compounds in this study shared a 1-(4-morpholinophenyl) prop-2-en-1-one structure. Introduction of various electron-donating and withdrawing groups onto the *para* position of the phenyl **B** ring of the basic chalcone scaffold afforded different derivatives. Surprisingly, unsubstituted **MO1** inhibited MAO-B more potently than the other eight derivatives. All nine derivatives exhibited MAO-B selectivity. In particular, **MO1** (IC₅₀ = 0.030 μM) was ~2 times more potent than the reversible MAO-B inhibitor lazabemide (IC₅₀ = 0.063 μM), and had a high selectivity index (SI = >1333.3), which meant that it was the best inhibitor in the series. Regarding MAO-B inhibition, **MO1** was slightly less potent than the reference irreversible MAO-B inhibitor pargyline (IC₅₀ = 0.028 μM). The presence of dimethylamino, chloro and bromo substituents at the *para* position of the chalcone **B** ring conferred moderate AChE inhibition. Recently, it was

reported that shifting of morpholine ring to the phenyl **B** ring of chalcones showed moderate AChE inhibition³⁵. Results of SAR analysis of MAO-B/AChE inhibitions by the nine compounds are provided in Figure 3.

2.2.2. Kinetics of MAO-B inhibition

Lineweaver–Burk plots and secondary plots of MAO-B inhibition by **MO1** showed that **MO1** is a mixed inhibitor of MAO-B ($K_i = 0.018 \pm 0.002$) (Figure 4(A,B)). These results suggested that **MO1** binds to an allosteric site other than the substrate-binding site of MAO-B.

2.2.3. Kinetics of AChE inhibitions

Lineweaver–Burk plots and secondary plots showed that **MO5** and **MO9** competitively and non-competitively, respectively, inhibited AChE (Figure 5(A,C)) with K_i values of 2.52 ± 0.17 and 7.04 ± 0.32 μM, respectively (Figure 5(B,D)), which suggest that **MO5** is a potent, selective and competitive inhibitor of AChE that binds to the active site of AChE, and that **MO9** binds to a site other than

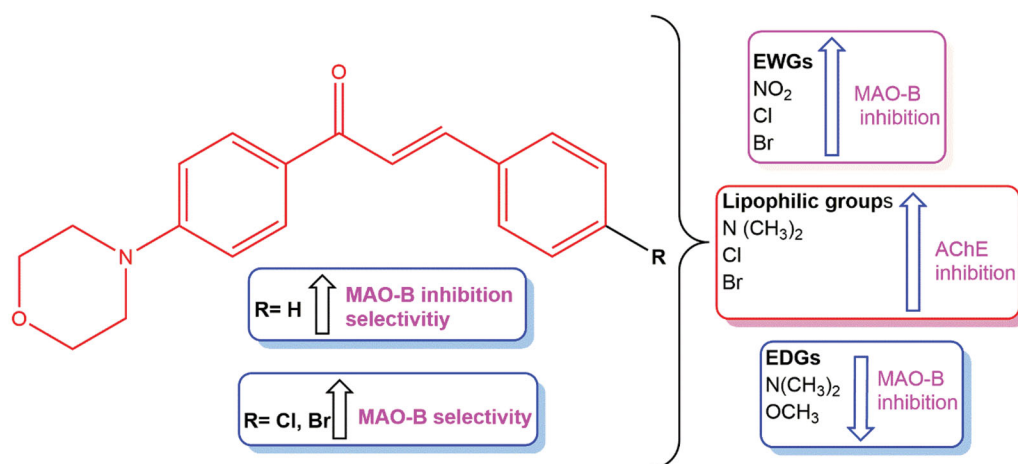


Figure 3. SAR analysis of MAO-B and AChE inhibitors.

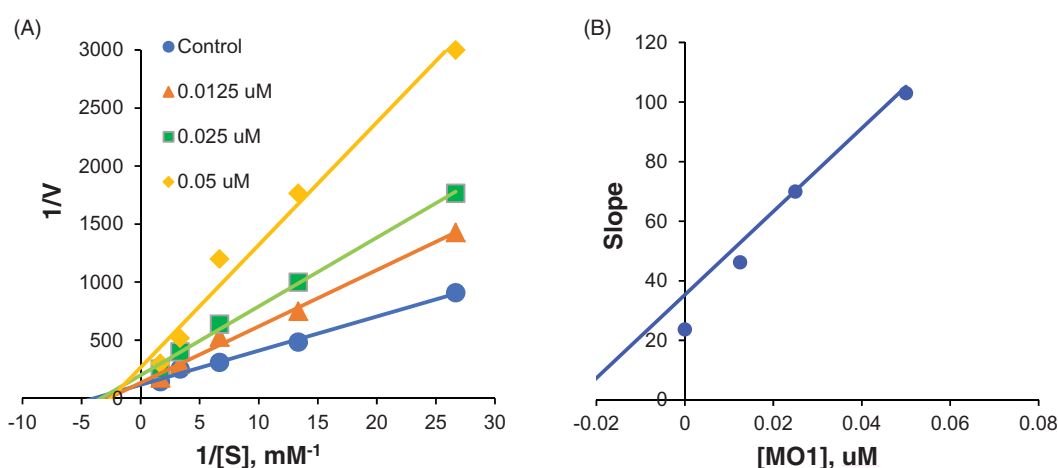


Figure 4. Lineweaver-Burk plots of MAO-B inhibition by **MO1** (A), and respective secondary plots (B) of slopes vs. inhibitor concentrations.

the active site of AChE and changes the 3D structure of the enzyme, thus inhibiting enzyme activity.

2.2.4. Analysis of the reversibilities of MAO-B and AChE inhibitions

Inhibition assays were carried out after preincubating MAO-B or AChE with the inhibitors for 15 min. The reversibilities of MAO-B inhibition by **MO1** and of AChE inhibitions by **MO5** and **MO9** were investigated by dialysis³⁴. Dialysis recovered the inhibition of MAO-B by **MO1** from 21.6% (A_U) to 77.1% (A_D), which was similar to that shown by lazabemide (from 38.8 to 90.0%), a reversible MAO-B inhibitor (Figure 6(A)). On the other hand, inhibition of MAO-B by pargyline (an irreversible inhibitor) was recovered from 10.7 to 16.5%. In addition, inhibitions of AChE by **MO5** and **MO9** were recovered by dialysis from 35.8% (A_U) to 79.2% (A_D) and from 33.8 to 80.7%, respectively, which were similar to that observed for tacrine (from 32.8 to 91.7%), a reversible AChE inhibitor (Figure 6(B)). These results indicate that **MO1** is a reversible inhibitor of MAO-B, and that **MO5** and **MO9** are reversible inhibitors of AChE.

2.3. Blood-brain barrier (BBB) permeation

The synthesised derivatives were screened for their abilities to cross the BBB using the parallel artificial membrane permeability assay (PAMPA) because this ability is a critical developmental requirement for any drug targeting neurodegenerative disorders

or depression. The PAMPA used was validated by comparing the experimentally determined permeabilities of eight commercial drugs with reported values (Table 2). According to reported BBB permeation limits, compounds were classified as follows:³⁶ CNS+ (high): $Pe (10^{-6} \text{ cm s}^{-1}) > 4.00$, CNS- (low): $Pe (10^{-6} \text{ cm s}^{-1}) < 2.00$ and CNS \pm (uncertain): $Pe (10^{-6} \text{ cm s}^{-1})$ from 4.00 to 2.00. Our results suggest that all nine synthesised derivatives could cross the BBB, and that **MO1**, **MO5** and **MO9** would be the most effective.

2.4. Cytotoxic studies

The biocompatibilities of **MO1**, **MO5** and **MO9** were investigated using an MTT (3-(4,5-dimethylthiazol-2-yl)-2,5-diphenyltetrazolium bromide) assay and normal VERO cells^{37,38}. Results showed that **MO1**, **MO5** and **MO9** were non-toxic to normal VERO cells with IC_{50} values of 195.14, 185.44 and 188.34 $\mu\text{g/mL}$, respectively, indicating that the therapeutic potentials of these compounds would be suitable.

2.5. Total ROSs assay

ROS are considered to be the radicals primarily responsible for the neuronal death observed in various neurodegenerative disorders³⁹. The lead compounds **MO1**, **MO5** and **MO9** were subjected to ROS assays using Hela cells. ROS levels significantly increased in

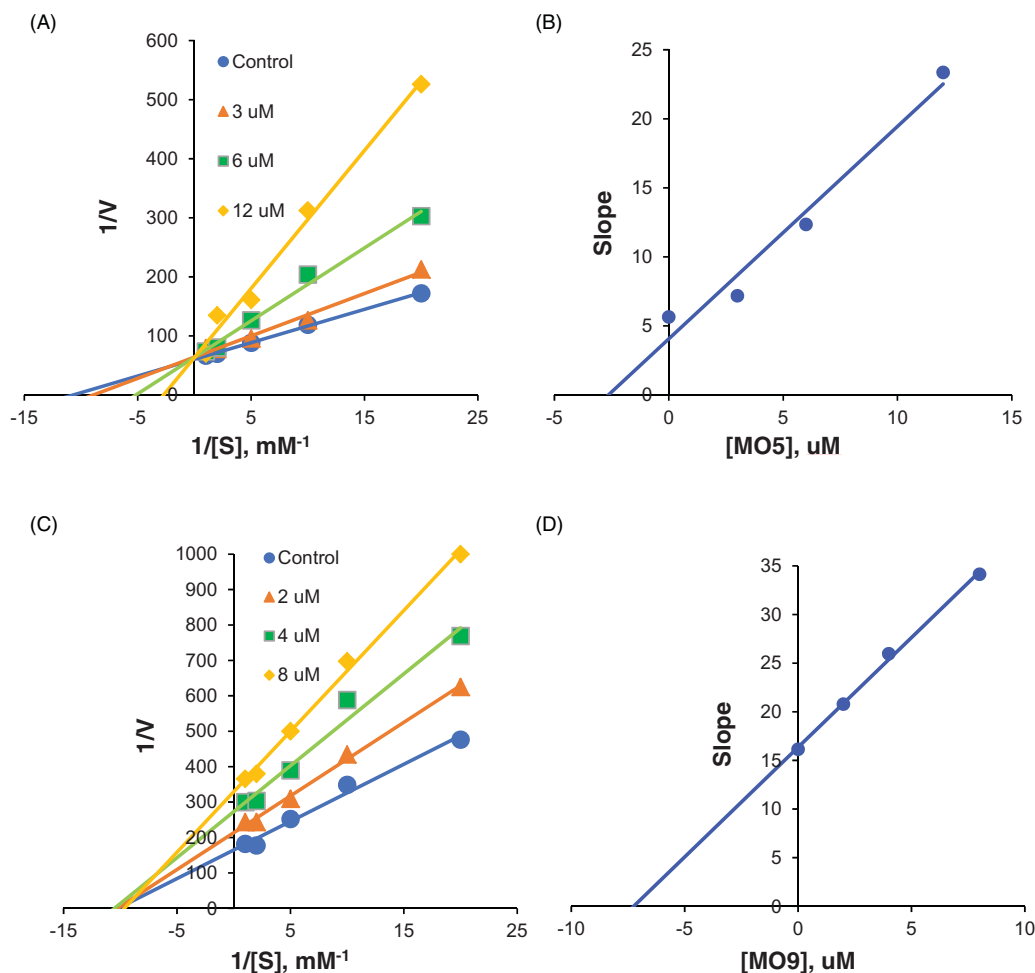


Figure 5. Lineweaver–Burk plots of AChE inhibition by **MO5** (A) and **MO9** (C), and respective secondary plots (B and D) of slopes vs. inhibitor concentrations.

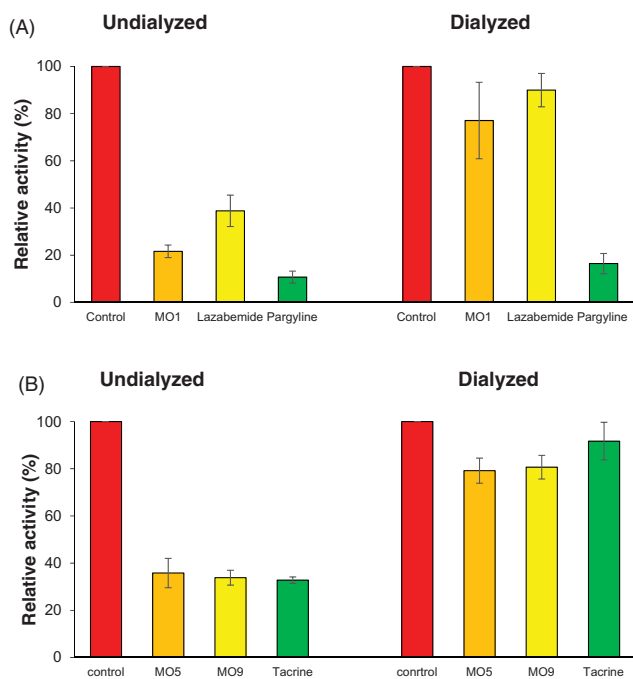


Figure 6. Dialysis recoveries of MAO-B inhibition by **MO1** (A) and AChE inhibition by **MO5** and **MO9** (B). The concentrations of the inhibitors used were approximately $2 \times IC_{50}$ values: **MO1**, 0.06 μM; **MO5**, 12.0 μM; **MO9**, 24.0 μM; lazabemide, 0.12 μM; pargyline, 0.06 μM; and tacrine, 0.54 μM (tacrine was used as a reference reversible inhibitor). For recovery experiments, preincubated enzyme mixtures were dialysed as described in the text.

Table 2. Experimental membrane permeabilities of the synthetic and reference inhibitors.

Compounds	Bibliography Pe ($\times 10^{-6}$ cm s ⁻¹)	Experimental Pe ($\times 10^{-6}$ cm s ⁻¹)	Prediction
Testosterone	17.0	16.86 ± 0.67	CNS+
Verapamil	16.0	15.69 ± 0.44	CNS+
β-estradiol	12.0	11.88 ± 0.53	CNS+
Progesterone	9.3	9.10 ± 0.11	CNS+
Piroxicam	2.5	2.35 ± 0.30	CNS+/-
Hydrocortisone	1.8	1.71 ± 0.05	CNS-
Lomefloxacin	1.1	1.26 ± 0.01	CNS-
Dopamine	0.2	0.21 ± 0.01	CNS-
MO1	—	16.34 ± 0.16	CNS+
MO5	—	14.44 ± 0.81	CNS+
MO9	—	14.61 ± 0.08	CNS+

H₂O₂-treated Hela cells as determined by fluorescent image analyses (Figure 7(B)). **MO1** and **MO5** (Figure 7(C,D)) at 40 μg/mL resulted in significantly lower ROS levels than **MO9** (Figure 7(E)). Interestingly, the colony formation induced by H₂O₂ was markedly reduced by the lead MAO-B inhibitor **MO1**, which suggested that the molecule can be highly recommended for the arrest of free radicals in the neurodegenerative disorders.

2.6. Computational studies

Initially, **MO1** and **MO5** were used as bases for profiling the pharmacological spectra of putative protein targets using the free web platform MuSSEL^{40,41}. Interestingly, MAO-B and AChE were

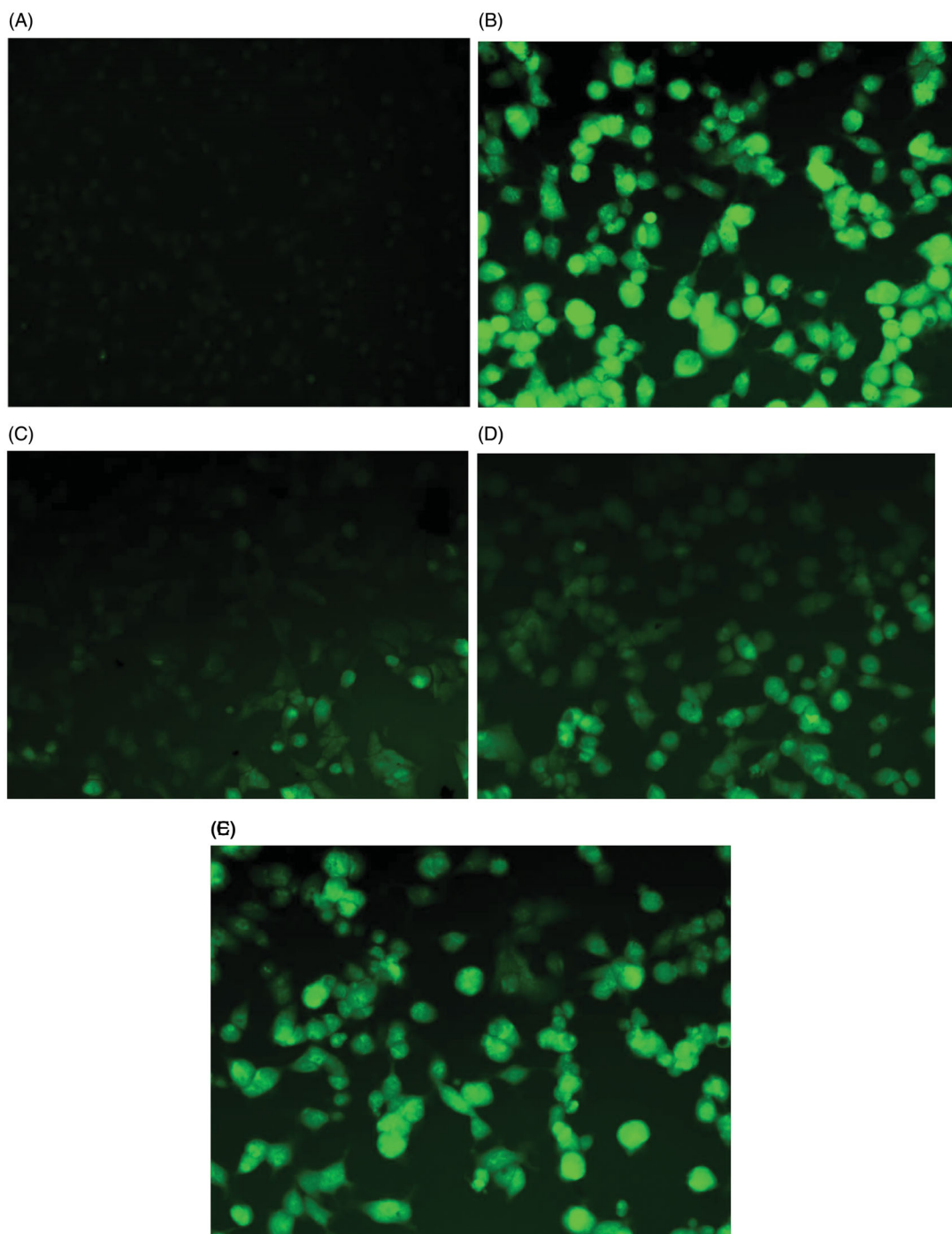


Figure 7. Inhibition of H_2O_2 -induced ROS generation in human cervical cancer cells. (A) Treatment-naïve control cells; (B) Cells treated with $100\ \mu\text{g/mL}$ of H_2O_2 ; (C) Cells treated with $40\ \mu\text{g/mL}$ of **MO1**; (D) Cells treated with $40\ \mu\text{g/mL}$ of **MO5**; (E) Cells- treated with $40\ \mu\text{g/mL}$ of **MO9**.

predicted to be 13th and 14th targets for **MO1** and 7th and 15th targets for **MO5**, respectively. Details are provided in Supporting Information.

Docking studies were performed on **MO1** and **MO5** using the X-ray resolved structures of MAO-A, MAO-B and AChE in the Protein Data Bank (PDB) as entries 2Z5X, 2VZ5 and 4EY7^{42–45}. Docking protocols were performed as we described in a previous study¹³. Molecular docking simulations were performed to investigate interactions between **MO1** and **MO5** and MAO-A, MAO-B and AChE. The docking scores resulting from *in silico* simulations are reported in Table 3. Results showed that the carbonyl and the 4-morpholin-phenyl groups of the chalcone scaffolds of **MO1** and

Table 3. Docking score values for bindings between **MO1** and **MO5** and MAO-B or AChE.

Compounds	Docking score (kcal/mol)		
	AChE	MAO-B	BChE
MO1	−10.31	−8.67	−7.42
MO5	−10.12	−9.34	−6.66

MO5 hydrogen-bonded with F295 and formed $\pi - \pi$ interactions with the side chain of W286 at the peripheral anionic subsite (PAS) of AChE (Figure 8(A)). Also, the dimethylamino group of **MO5** established a weak hydrophobic interaction with W86 at the

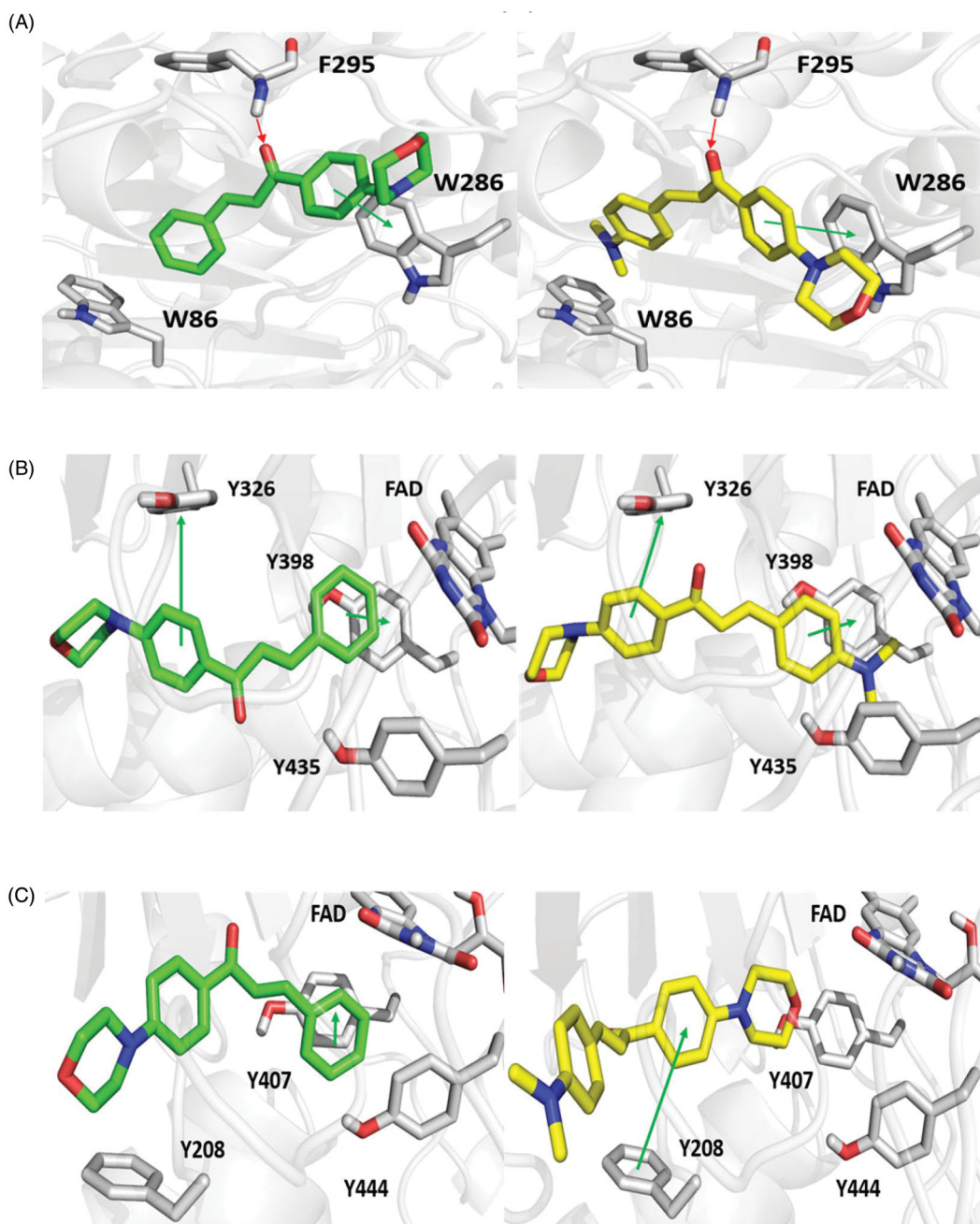


Figure 8. Top scored poses of **MO1** and **MO5** for binding with AChE (A), MAO-B (B) and MAO-A (C) are shown on left and right sides, respectively. **MO1**, **MO5** and key enzyme residues are displayed as green, yellow and grey sticks, respectively. Green and red arrows indicate π - π interactions and hydrogen bonds, respectively.

catalytic anionic subsite (CAS). **MO1** and **MO5** formed π - π interactions with the selective MAO-B residue Y326 (Figure 8(B)). In addition, the styryl and dimethylaminophenyl groups of **MO1** and **MO5**, respectively, established π - π interactions with Y398 and were sandwiched within an aromatic cage formed by Y328, Y435 and FAD. **MO1** engaged in a π - π interaction with Y407 and was entangled in a hydrophobic cage consisting of Y407, Y444 and FAD of MAO-A (Figure 8(C)), whereas **MO5** established π - π interactions with a selective MAO-A residue F208 using its 4-morpholine-phenyl group. In order to point out the selectivity of **MO1** and **MO5**, molecular docking analyses were performed on BChE crystal structure. Docking score values of **MO1** and **MO5** for BChE were worse than those for AChE (Table 3). Interestingly, **MO1** and **MO5** can predominantly establish hydrophobic interactions in the

BChE binding pocket; in particular **MO1** engaged a π - π interaction with F329, but both compounds cannot make crucial interactions with the catalytic W82 residue (Figure 8(D)).

Overall, computational analyses provided a sound explanation of the experimental data. Docking scores and the binding modes obtained demonstrated that **MO1** and **MO5** can meaningfully interact with MAO-B as indicated by IC_{50} experimental values. Interestingly, even if **MO1** had adopted a similar binding mode in MAO-A and MAO-B binding pockets, the two docking score values would have been quite different, due to a lack of π - π interaction with the MAO-A selective residue F208 and lesser hydrophobic interactions. On the other hand, **MO5** assumed a switched pose within the MAO-A binding pocket, with its morpholine ring facing FAD, presumably because the dimethylamino

substituent on the phenyl ring did not allow adequate access to the binding site. As regards AChE, molecular docking awarded a better score for **MO5** than **MO1**, which also agreed with experimental data, despite the resemblance between their binding poses.

3. Conclusion

We describe the synthesis of morpholine-containing α,β -unsaturated ketones, and the results of an investigation of their MAOs and AChE inhibition profiles. Most of the nine compounds synthesised exhibited potent MAO-B inhibition with moderate AChE inhibition. Interestingly, **MO1** (the lead compound) inhibited MAO-B inhibition in the low nanomolar range and was more potent than lazabemide (the reference compound). The low cytotoxicity and the ability of **MO1** to transit the BBB support our drug design strategy. In addition, the ROS scavenging efficacy of **MO1** suggests improved neuroprotective effects.

4. Experimental

4.1. Enzyme assays

MAO-A activity was measured continuously for 20 min at 316 nm using 0.06 mM kynuramine as substrate, as described previously^{46,47}, whereas MAO-B activity was measured for 30 min at 250 nm using 0.3 mM benzylamine as substrate. MAO activity assays were performed using recombinant human MAO-A or MAO-B. A slightly modified version of the method developed by Ellman⁴⁸ was used to measure AChE and BChE activities, using 0.5 mM acetylthiocholine iodide (ATCI) and *S*-butyrylthiocholine iodide (BTCI), respectively, as substrates for 10 min at 412 nm⁴⁹. Colour development was performed using 0.5 mM 5,5'-dithiobis (2-nitrobenzoic acid) (DTNB), which reacts with thiocholine (a product of ATCI by AChE or of BTCI by BChE) to produce 5-thio 2-nitrobenzoic acid. Preincubation was treated for 15 min before adding ATCI and DTNB.

4.2. Analysis of enzyme inhibitions and kinetics

MAO-A, MAO-B, AChE and BChE activities were measured after exposure to inhibitors at a concentration of 10 μ M. Inhibitions of MAO-B at 10 μ M of these compounds tested were too excessive, and thus, a concentration of 1.0 μ M was used. IC₅₀ values were determined by measuring the residual enzyme activities. Toloxatone, lazabemide and tacrine, were used as reference reversible inhibitors of MAO-A, MAO-B and AChE, respectively, and cloglyline and pargyline as reference irreversible inhibitors of MAO-A and MAO-B, respectively. K_i values and inhibitor types were determined by kinetic testing, as previously described⁵⁰. Kinetic tests were conducted at 5 different substrate concentrations, and the inhibitor concentrations used were 0, $\sim 1/2 \times$ IC₅₀, IC₅₀, and $2 \times$ IC₅₀ values. Lineweaver–Burk plots and their secondary plots were used to determine K_i values and inhibitor types.

4.3. Analysis of inhibitor reversibilities

Inhibition types (reversible or irreversible) were determined by dialysis, as previously described^{51,52}, but by using 0.06 mM kynuramine and 0.3 mM benzylamine. For the experiment of AChE, 0.5 mM ATCI was used. Dialysis experiments were performed by preincubating enzymes and inhibitors (or reference inhibitors) at $\sim 2 \times$ IC₅₀ in 0.1 M sodium phosphate buffer (pH 7.2) for 30 min,

and then dialysing solutions with stirring for 6 h with a buffer change at 3 h. Residual activities were calculated using the measured activities of undialysed (A_U) and dialysed (A_D) solutions and the activities of untreated controls (i.e. without inhibitor).

Disclosure statement

No potential conflict of interest was reported by the authors.

Funding

This research was supported by the National Research Foundation of Korea (NRF) grant funded by the Republic of Korea government (Grant No. NRF-2019R1A2C1088967 to H. Kim).

ORCID

Hoon Kim  <http://orcid.org/0000-0002-7203-3712>

References

- Rodríguez-Soacha DA, Scheiner M, Decker M. Multi-target-directed-ligands acting as enzyme inhibitors and receptor ligands. *Eur J Med Chem* 2019;180:690–706.
- Zhang P, Xu S, Zhu Z, Xu J. Multi-target design strategies for the improved treatment of Alzheimer's disease. *Eur J Med Chem* 2019;176:228–47.
- Silva MF, Dias KST, Gontijo VS, et al. Multi-target directed drugs as a modern approach for drug design towards Alzheimer's disease: an update. *Curr Med Chem* 2018;25:3491–525.
- Youdim MBH, Buccafusco JJ. Multi-functional drugs for various CNS targets in the treatment of neurodegenerative disorders. *Trends Pharmacol Sci* 2005;26:27–35.
- Carradori S, Silvestri R. New frontiers in selective human MAO-B inhibitors. *J Med Chem* 2015;58:6717–32.
- Rehuman NA, Mathew B, Jat RK, et al. A comprehensive review of monoamine oxidase-A inhibitors in their syntheses and potencies. *Comb Chem High Throughput Screen* 2020;23:898–914.
- Mathew B, Parambi DGT, Mathew GE, et al. Emerging therapeutic potentials of dual-acting MAO and AChE inhibitors in Alzheimer's and Parkinson's diseases. *Arch Pharm (Weinheim)* 2019;352:e1900177.
- Zhang HY. One-compound-multiple-targets strategy to combat Alzheimer's disease. *FEBS Lett* 2005;579:5260–4.
- Carradori S, Ortuso F, Petzer A, et al. Design, synthesis and biochemical evaluation of novel multi-target inhibitors as potential anti-Parkinson agents. *Eur J Med Chem* 2018;143:1543–52.
- Secci D, Carradori S, Petzer A, et al. 4-(3-Nitrophenyl)thiazol-2-ylhydrazone derivatives as antioxidants and selective hMAO-B inhibitors: synthesis, biological activity and computational analysis. *J Enzyme Inhib Med Chem* 2019;34:597–612.
- Tzara A, Xanthopoulos D, Kourounakis AP. Morpholine as a scaffold in medicinal chemistry: An update on synthetic strategies. *ChemMedChem* 2020;15:392–403.
- Kourounakis AP, Xanthopoulos D, Tzara A. Morpholine as a privileged structure: a review on the medicinal chemistry

- and pharmacological activity of morpholine containing bioactive molecules. *Med Res Rev* 2020;40:709–52.
13. Reeta Baek SC, Lee JP, Rangarajan TM, et al. Ethyl acetohydroxamate incorporated chalcones: Unveiling a novel class of chalcones for multitarget monoamine oxidase-B inhibitors against Alzheimer's disease. *CNS Neurol Disord Drug Targets* 2019;18:643–54.
 14. Guglielmi P, Mathew B, Secci D, Carradori S. Chalcones: unearthing their therapeutic possibility as monoamine oxidase B inhibitors. *Eur J Med Chem* 2020;205:112650.
 15. Mathew B, Parambi DGT, Sivasankarapillai Uddin MS, et al. Perspective design of chalcones for the management of CNS disorders: a mini-review. *CNS Neurol Disord Drug Targets* 2019;18:432–45.
 16. Zhuang C, Zhang W, Sheng C, et al. Chalcone: a privileged structure in medicinal chemistry. *Chem Rev* 2017;117:7762–810.
 17. Mathew B, Haridas A, Suresh J, et al. Monoamine oxidase inhibitory action of chalcones: a mini review. *Cent Nerv Syst Agents Med Chem* 2016;16:120–36.
 18. Chimenti F, Fioravanti R, Bolasco A, et al. Chalcones: a valid scaffold for monoamine oxidases inhibitors. *J Med Chem* 2009;52:2818–24.
 19. Mathew B, Mathew GE, Uçar G, et al. Development of fluorinated methoxylated chalcones as selective monoamine oxidase-B inhibitors: synthesis, biochemistry and molecular docking studies. *Bioorg Chem* 2015; 62:22–9.
 20. Mathew B, Uçar G, Mathew GE, et al. Monoamine oxidase inhibitory activity: methyl-versus chlorochalcone derivatives. *Chem Med Chem* 2016;11:2649–55.
 21. Mathew B, Haridas A, Uçar G, et al. Synthesis, biochemistry, and computational studies of brominated thienyl chalcones: a new class of reversible MAO-B inhibitors. *Chem Med Chem* 2016;11:1161–71.
 22. Hammuda A, Shalaby R, Rovida S, et al. Design and synthesis of novel chalcones as potent selective monoamine oxidase-B inhibitors. *Eur J Med Chem* 2016;114:162–9.
 23. Parambi DGT, Oh JM, Baek SC, et al. Design, synthesis and biological evaluation of oxygenated chalcones as potent and selective MAO-B inhibitors. *Bioorg Chem* 2019;93:103335.
 24. Lakshminarayan B, Baek SC, Kannappan N, et al. Ethoxylated head of chalcones as a new class of multi-targeted MAO inhibitors. *Chem Select* 2019;4:6614–9.
 25. Shalaby R, Petzer JP, Petzer A, et al. SAR and molecular mechanism studies of monoamine oxidase inhibition by selected chalcone analogs. *J Enzyme Inhib Med Chem* 2019; 34:863–76.
 26. Kong Z, Sun D, Jiang Y, Hu Y. Design, synthesis, and evaluation of 1, 4-benzodioxan-substituted chalcones as selective and reversible inhibitors of human monoamine oxidase B. *J Enzyme Inhib Med Chem* 2020;35:1513–25.
 27. Oh JM, Rangarajan TM, Reeta C, et al. Novel class of chalcone oxime ethers as potent monoamine oxidase-B and acetylcholinesterase inhibitors. *Molecules* 2020;20:2536.
 28. Wang L, Wang Y, Tian Y, et al. Design, synthesis, biological evaluation, and molecular modeling studies of chalcone-rivastigmine hybrids as cholinesterase inhibitors. *Bioorg Med Chem* 2017;25:360–71.
 29. Xiao G, Li Y, Qiang X, et al. Design, synthesis and biological evaluation of 4'-aminochalcone-rivastigmine hybrids as multifunctional agents for the treatment of Alzheimer's disease. *Bioorg Med Chem* 2017;25:1030–41.
 30. Cao Z, Yang J, Xu R, et al. Design, synthesis and evaluation of 4'-OH-flurbiprofen-chalcone hybrids as potential multifunctional agents for Alzheimer's disease treatment. *Bioorg Med Chem* 2018;26:1102–15.
 31. Tian C, Qiang X, Song Q, et al. Flurbiprofen-chalcone hybrid mannich base derivatives as balanced multifunctional agents against Alzheimer's disease: design, synthesis and biological evaluation. *Bioorg Chem* 2020;94:103447.
 32. Mathew B. Privileged pharmacophore of FDA approved drugs in combination with chalcone framework: a new hope for Alzheimer's treatment. *Comb Chem High Throughput Screen* 2020;23:842–846.
 33. Mathew B, Baek SC, Parambi DGT, et al. Potent and highly selective dual-targeting monoamine oxidase-B inhibitors: fluorinated chalcones of morpholine versus imidazole. *Arch Pharm* 2019;352:e1800309.
 34. Maliyakkal N, Eom BH, Heo JH, et al. A new potent and selective monoamine oxidase-B inhibitor with extended conjugation in a chalcone framework: 1-[4-(morpholin-4-yl)phenyl]-5-phenylpenta-2,4-dien-1-one. *ChemMedChem* 2020;15:1629–33.
 35. Polo E, Nicol Ibarra-Arellano N, Prent-Penalozaa L, et al. Ultrasound-assisted synthesis of novel chalcone, heterochalcone and bis-chalcone derivatives and the evaluation of their antioxidant properties and as acetylcholinesterase inhibitors. *Bioorg Chem* 2019;90:103034.
 36. Di L, Kerns EH, Fan K, et al. High throughput artificial membrane permeability assay for blood-brain barrier. *Eur J Med Chem* 2003;38:223–32.
 37. Suresh J, Baek SC, Ramakrishnan SP, et al. Discovery of potent and reversible MAO-B inhibitors as furanochalcones. *Int J Biol Macromol* 2018;108:660–4.
 38. Dev S, Parambi DGT, Baby B, et al. An environment-friendly synthesis of piperonal chalcones and their cytotoxic and antioxidant evaluation. *Lett Drug Des Drug Discov* 2020;17:138–44.
 39. Park C, Cha HJ, Hong SH, et al. Protective effects of phloroglucinol on oxidative stress-induced DNA damage and apoptosis through activation of the Nrf2/HO-1 signaling pathway in HaCaT human keratinocytes. *Mar Drugs* 2019;17:225.
 40. Montaruli M, Alberga D, Ciriaco F, et al. Accelerating drug discovery by early protein drug target prediction based on multi-fingerprint similarity search. *Molecules* 2019;24:2233.
 41. Alberga D, Trisciuzzi D, Montaruli M, et al. A new approach for drug target and bioactivity prediction: the multifingerprint similarity search algorithm (MuSSeL). *J Chem Inf Model* 2019;59:586–96.
 42. Son SY, Ma J, Kondou Y, et al. Structure of human monoamine oxidase A at 2.2-Å resolution: the control of opening the entry for substrates/inhibitors. *Proc Natl Acad Sci USA* 2008;105:5739–44.
 43. Binda C, Wang J, Pisani L, et al. Structures of human monoamine oxidase B complexes with selective noncovalent inhibitors: safinamide and coumarin analogs. *J Med Chem* 2007;50:5848–52.
 44. Cheung J, Rudolph MJ, Burshteyn F, et al. Structures of human acetylcholinesterase in complex with pharmacologically important ligands. *J Med Chem* 2012;55:10282–6.

45. Kořak U, Brus B, Knez D, et al. Development of an in-vivo active reversible butyrylcholinesterase inhibitor. *Sci Rep* 2016;6:39495
46. Mathew B, Baek SC, Grace Thomas Parambi D, et al. Selected aryl thiosemicarbazones as a new class of multi-targeted monoamine oxidase inhibitors. *MedChemComm* 2018; 9:1871–81.
47. Baek SC, Park MH, Ryu HW, et al. Rhamnocitrin isolated from *Prunus padus* var. *seoulensis*: a potent and selective reversible inhibitor of human monoamine oxidase A. *Bioorg Chem* 2018;28:317–25.
48. Ellman GL, Courtney KD, Andres V, Jr, Feather-Stone RM. A new and rapid colorimetric determination of acetylcholinesterase activity. *Biochem Pharmacol* 1961;7:88–95.
49. Lee JP, Kang MG, Lee JY, et al. Potent inhibition of acetylcholinesterase by sargachromanol I from *Sargassum siliquastrum* and by selected natural compounds. *Bioorg Chem* 2019;89:103043.
50. Lee HW, Ryu HW, Kang MG, et al. Potent selective monoamine oxidase B inhibition by maackiain, a pterocarpan from the roots of *Sophora flavescens*. *Bioorg Med Chem Lett* 2016;26:4714–9.
51. Baek SC, Lee HW, Ryu HW, et al. Selective inhibition of monoamine oxidase A by hispidol. *Bioorg Med Chem Lett* 2018;15:58–588.
52. Sasidharan R, Baek SC, Manju SL, et al. Imidazole bearing chalcones as a new class of monoamine oxidase inhibitors. *Biomed Pharmacother* 2018;106:8–13.